

Imaging of marine seismic data

Marlon S. Mota¹, Jozinei F. Lopes², Raimundo N. C. Carneiro¹, Felipe A. V. Pena², Raphael Di Carlo S. dos Santos¹ and Suelen C. Fernandes¹

¹UFOPA, Santarém, Brazil

²UFPA, Belém, Brazil

Copyright 2019, SBGf - Sociedade Brasileira de Geofísica.

This paper was prepared for presentation at the 16th International Congress of the Brazilian Geophysical Society, held in Rio de Janeiro, Brazil, August 19-22, 2019.

Contents of this paper were reviewed by the Technical Committee of the 16th International Congress of The Brazilian Geophysical Society and do not necessarily represent any position of the SBGf, its officers or members. Electronic reproduction or storage of any part of this paper for commercial purposes without the written consent of The Brazilian Geophysical Society is prohibited.

Resumo

The present work aims the processing and imaging of the AMOCO marine seismic data using the NMO methodology to construct of velocity model based in the analysis of the semblance map. Migrated sections were obtained in time.

Introduction

The exploration of marine energy resources requires high technology for success and optimization of costs. In this way, the academy and projects with economic resources directed to develop research and to contribute to the formation of Human resources for oil and gas. Thus the field of geophysical exploration, particularly the seismic method, has a fundamental role in obtaining images of sedimentary basin reducing the exploratory risk. The use of the NMO methodology has the purpose of complementing and increasing the information about the features of the subsurface. The main results are stacked and migrated sections are discussed in more detail in the sequence of the work. For the processing and imaging the applications were used CWP/Un*x (Forel et al., 2005; Cohen and Stockwell, 2005).

Acquisition parameters

The seismic data using in this processing is the AMOCO dataset. The strategy that was followed in this work is shown in the figure 1, and the acquisition parameters of data are shown in table 1.

Figure 2 shows minimum-offset data with application of mute before preprocessing steps.

Figure 3 shows the offset-minimum of data after application of filtering f , $f - k$ and spheric divergence correction to attenuate low and high noise recovering amplitudes which decay quickly.

NMO method

The methodology consists of specific steps and organized with titles of NMO method. A common property to these two methods is the use common-mid-point (CMP) gathers,

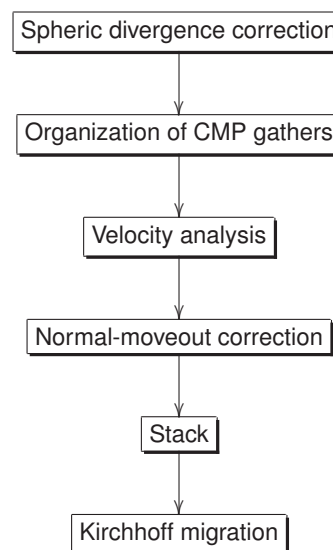


Figura 1: NMO stacking flowchart.

Tabela 1: Acquisition parameters.

Shot and receiver geometry	
shot number	385
shot interval	50 m
receiver number	256
receiver interval	25 m

CMP geometry	
CMP number	1792
CMP interval	12,5 m
maximum coverage	64

Record parameters	
Record time	3,5 s
sample interval	9,9 ms

that are characterized by the source-sensor reciprocity principle, and consequently not solving for tilted reflectors. Another common property is the semblance measure of coherence along the trajectories, $t(h)$ and $t(x_m, h)$, of the sum of traces to produce the stack CMP sections.

This work uses the normal-moveout (NMO) correction and stack based on a model by flat, homogeneous and isotropic layers, where the primary traveltime is given by

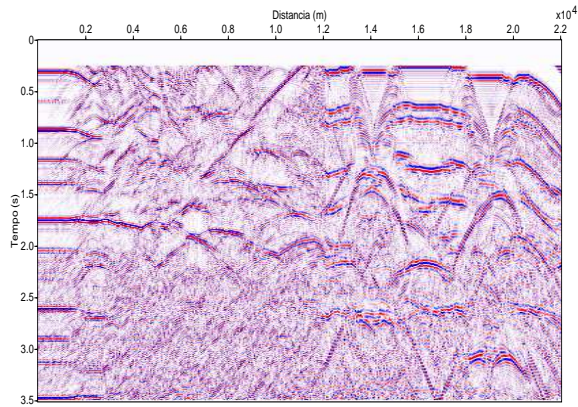


Figure 2: Minimum offset before application of the filters f and $f-k$.

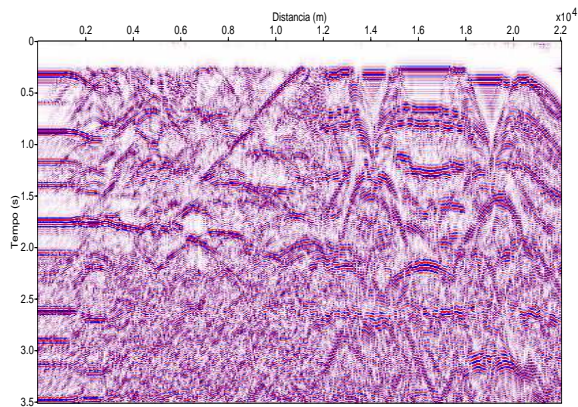


Figure 3: Minimum offset after filtering f , $f-k$ and spheric divergen correction. It is observed sensitive resolution increasing of sesismic events.

the hyperbolic approximation (1) (Hubral and Krey, 1980):

$$t(h) = \sqrt{t^2(0) + \frac{(2h)^2}{v^2}}; \quad (1)$$

where the independent variable h is the half-offset of the source-receiver pair; $t(0)$ is the traveltim relative to the normal incidence in zero offset; v is the search parameter, where $v = v_{\text{NMO}}$ defines a velocity for the normal-moveout time correction, stack and to estimate the v_{RMS} velocity (root mean square). Therefore, this model is to be considered as initial, since it only considers vertical variation of velocity within the aperture established for the calculation. A next more complex model considers layers with dipping interfaces, but still admitting CMP gathers and the semblance measure.

In the NMO case, the analysis of the v parameter is performed based on the CMP gathers by picking pairs of (v_{NMO}, t_0) in the semblance coherence section calculated with equation (2), where the values of $S(t_0, \mathbf{m})$ vary in the

range $(0, 1)$ (Sguazzero and Vesnaver, 1987):

$$S(t_0, \mathbf{m}) = \frac{1}{N} \frac{\sum_{t=t_0-\delta t/2}^{t_0+\delta t/2} \left[\sum_{h=h_1}^{h_2} \bar{u}(h, t; t_0, \mathbf{m}) \right]^2}{\sum_{t=t_0-\delta t/2}^{t_0+\delta t/2} \sum_{h=h_1}^{h_2} [\bar{u}(h, t; t_0, \mathbf{m})]^2}, \quad (2)$$

where $\bar{u}(h, t; t_0, \mathbf{m})$ represents the processed trace amplitude positioned along the path of the subtended sum of equation (1); N is the number of involved traces; \mathbf{m} is the trajectory function parameters vector, $t(h; t_0, \mathbf{m})$. The sum along $t(h)$ and is defined within a spatial-temporal window where is selected a curve that best represents the reflection event. In the NMO case, the search parameter is only the velocity named $v = \mathbf{m} = v_{\text{NMO}}$ that, depending on the application, can be expressed mathematically by the v_{RMS} velocity.

Stacking is done for each CMP gather through the expression

$$\bar{s}_{t_0} = \frac{1}{N} \sum_{i=0}^N \bar{u}_{i, t_i}; \quad (3)$$

where \bar{s}_{t_0} is the resultant amplitude of stack; \bar{u}_{i, t_i} is the amplitude in i -esimo trace in double-time t_i ; and N is the number of traces to be stacked in each CMP gather.

Kirchhoff time migration

Migration is described from the solution of scalar wave equation with constant density, given by:

$$\nabla^2 u(\vec{r}, t) - \frac{1}{c^2} \frac{\partial^2 u(\vec{r}, t)}{\partial t^2} = -4\pi q(\vec{r}, t), \quad (4)$$

where $u(\vec{r}, t)$ is the amplitude of field, c is the velocity of medium, $q(\vec{r}, t)$ is the source and $\vec{r} = (x, y, z)$ is point of observation.

The solution to Eq. (4) without source, considering one volume V_0 delimited for a surface S_0 , is given by Grenn Theorem (Schneider, 1978):

$$u(\vec{r}, t) = \frac{1}{4\pi} \int_{t_0} dt_0 \int_{S_0} dS_0 \left[G \frac{\partial}{\partial n} u(\vec{r}_0, t_0) - u(\vec{r}_0, t_0) \frac{\partial}{\partial n} G \right]; \quad (5)$$

where $\vec{n} = n\hat{n}$ is the normal vector surface S_0 , which include the aquisition surface A_0 , and the surface semi-spherica A' which is extrapolated for infinite so that their contribution is negligible (see Figure 4). Thus, the frontier is expressed by integral in superface of aquisition, end the solution is based in Green function which consists of response of a puntual source in \vec{r}_0 and its image in \vec{r}'_0 , given by:

$$G(\vec{r}, t | \vec{r}_0, t_0) = \frac{\delta(t - t_0 - \frac{R}{c})}{R} - \frac{\delta(t - t_0 - \frac{R'}{c})}{R'}, \quad (6)$$

where

$$R = [(x - x_0)^2 + (y - y_0)^2 + (z - z_0)^2]^{\frac{1}{2}}, \quad (7)$$

$$R' = [(x - x_0)^2 + (y - y_0)^2 + (z + z_0)^2]^{\frac{1}{2}}. \quad (8)$$

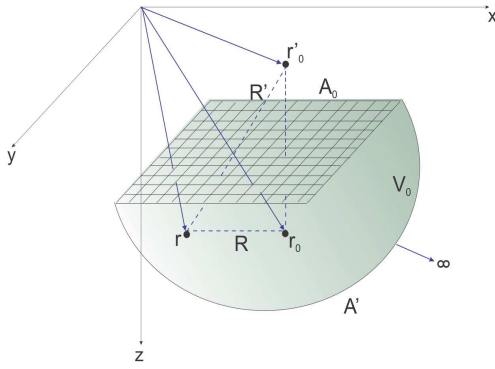


Figura 4: Scalar medium (3D) with volume V_0 delimited by the frontier $S_0 = A_0 + A'$, with one source point in \vec{r}'_0 , its image in \vec{r}'_0 and one observation point in \vec{r} (Schneider, 1978).

The field $u(\vec{r}_0, t_0)$ is measured in frontier $S_0 = A_0 + A'$, where the Green function is canceled ($G = 0$), and the component $\frac{\partial u(\vec{r}_0, t_0)}{\partial n}$ is canceled. With this, the equation (5) is simplified in form:

$$u(\vec{r}, t) = \frac{1}{2\pi} \int_{t_0} dt_0 \int_{A_0} dA_0 \left\{ u(\vec{r}_0, t_0) \frac{\partial}{\partial z_0} \left[\frac{\delta(t - t_0 - \frac{R}{c})}{R} \right] \right\}. \quad (9)$$

Switching $\frac{\partial}{\partial z_0}$ for $\frac{\partial}{\partial z}$ and resolving the temporal part of equation (9), it gets:

$$u(\vec{r}, t) = -\frac{1}{\pi} \frac{\partial}{\partial z} \int_{A_0} dA_0 \frac{u(\vec{r}_0, t - \frac{R}{c})}{R}. \quad (10)$$

This representation indicates which the Eq.(5) is solution of wave equation of form $\frac{f(t - \frac{R}{c})}{R}$ in integrating.

Results

Figure 5 shows the semblance map where the pairs (v_{NMO}, t_0) should be picked together with analysis of reflection events, and each one is related with one pair which better flat the event.

Figure 6 showing the before and after the NMO correction, using the velocity model obtained by analysis of coherence semblance.

Figure 7 shows the NMO velocity model time used in NMO stack. Figure 8 shows the stacked section that also used the velocity model of Figure 7.

The post-stack Kirchhoff time migration (Figure 9) was performed using the velocity model $v_{RMS}(t)$ shown in Figure 7 obtained during the velocity analysis in semblance map. Analyzing this section (see Figure 9) it is noticed that the subsurface structures do not change considerably their location in comparison the stacked section shows in Figure 8. The advantages of analysis of this migrated section is the identification of structures little perceived in stacked section, in which it is notable the better continuity of the reflecting interfaces.

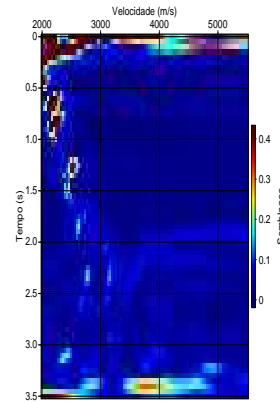


Figura 5: Semblance map for CMP 1150.

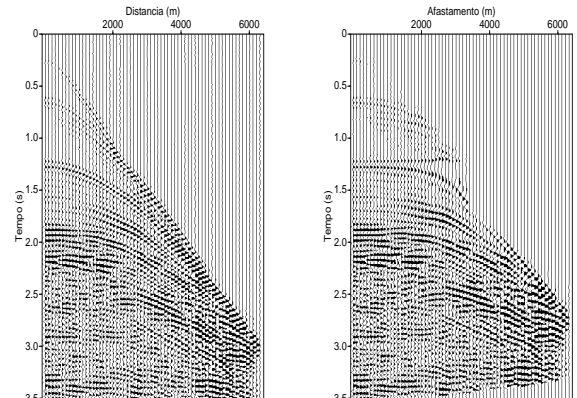


Figura 6: CMP 150 before (left), and after the NMO correction (right).

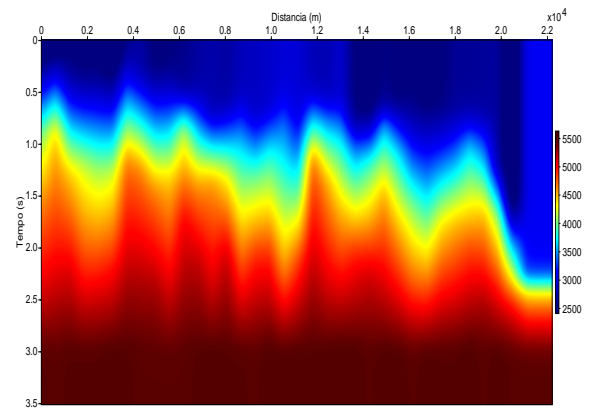


Figura 7: Velocity time model.

Conclusions

The velocity analysis was performed in the semblance map for reflection events. The velocity model is presented in Figure 7, where we observe the structure of the marine data. In the stack section shown in Figure 8 we observe a meaningful increase in the signal-to-noise ratio.

A post-stack Kirchhoff time migration shown in Figure 9 was obtained from the stack section of Figure 8 using the velocity model of Figure 7. The results pointed for the partial collapse of some diffraction events and the recovering of depth reflection events. Also undesirable are

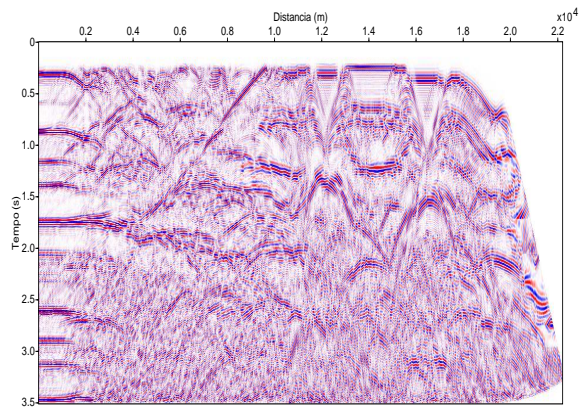


Figura 8: NMO stacked section.

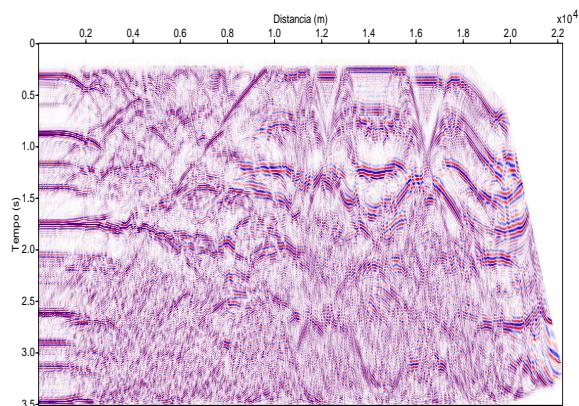


Figura 9: Kirchhoff time-migrated section

shape events are present in the deeper parts of the section.

As suggestions for future work we propose the application of depth migration based on equation such as Kirchhoff, PSPI (PhaseShift Plus Interpolation), SS (Split-Step), RTM (Reverse Time Migration), and FFD (Fourier Finite Difference), for comparison with the Kirchhoff time migration time stack and the generalization and the application of the CRS stack.

Acknowledgments

The authors would like to thank the Geosciences Engineering Institute of UFOPA and SBGf. The thanks are also extended to CAPES for the scholarship.

Referências

Cohen, J. K., and Stockwell, J. J. W., 2005, Seismic un*x release n. 39: Center for Wave Phenomena, Colorado School of Mines, Colorado.

Forel, D., Benz, T., and Pennington, W. D., 2005, Seismic data processing with seismic un*x - a 2d seismic data processing primer., volume 12 Society of Exploration Geophysicists.

Hubral, P., and Krey, T., 1980, Interval velocities from seismic reflection time measurements: Society of Exploration Geophysicists, Tulsa, OK.

Schneider, W. A., 1978, Integral formulation for migration in

two-dimensions and three-dimensions:, **43**, no. 01, 49–76.

Sguazzero, P., and Vesnaver, A., 1987, A comparative analysis of algorithms for stacking velocity estimation: Deconvolution and inversion: Blackwell Scientific Publications, Oxford.